University of Reading

Aerosol-forced AMOC changes in CMIP6 historical simulations

Article

Published Version

Creative Commons: Attribution 4.0 (CC-BY)

Open Access

Menary, M. B., Robson, J. ORCID: https://orcid.org/0000-0002-3467-018X, Allan, R. ORCID: https://orcid.org/0000-0003-0264-9447, Booth, B. B. B., Cassou, C., Gastineau, G., Gregory, J., Hodson, D. ORCID: https://orcid.org/0000-0001-7159-6700, Jones, C., Mignot, J., Ringer, M., Sutton, R. ORCID: https://orcid.org/0000-0001-8345-8583, Wilcox, L. ORCID: https://orcid.org/0000-0001-5691-1493 and Zhang, R. (2020) Aerosol-forced AMOC changes in CMIP6 historical simulations. Geophysical Research Letters. e2020GL088166. ISSN 0094-8276 doi: https://doi.org/10.1029/2020GL088166 Available at https://centaur.reading.ac.uk/91305/

It is advisable to refer to the publisher's version if you intend to cite from the work. See Guidance on citing.

To link to this article DOI: http://dx.doi.org/10.1029/2020GL088166

Publisher: American Geophysical Union

All outputs in CentAUR are protected by Intellectual Property Rights law, including copyright law. Copyright and IPR is retained by the creators or other copyright holders. Terms and conditions for use of this material are defined in the End User Agreement.

www.reading.ac.uk/centaur

CentAUR

Central Archive at the University of Reading

Reading's research outputs online

Geophysical Research Letters

RESEARCH LETTER
10.1029/2020GL088166

Aerosol-Forced AMOC Changes in CMIP6 Historical Simulations

Matthew B. Menary[1], Jon Robson[2], Richard P. Allan[3], Ben B. B. Booth[4], Christophe Cassou[5], Guillaume Gastineau[1], Jonathan Gregory[2,4], Dan Hodson[2], Colin Jones[6], Juliette Mignot[1], Mark Ringer[4], Rowan Sutton[2], Laura Wilcox[2], and Rong Zhang[7]

[1]LOCEAN, Sorbonne Université, Paris, France, [2]NCAS, Department of Meteorology, University of Reading, Reading, UK, [3]National Centre for Earth Observation, Department of Meteorology, University of Reading, Reading, UK, [4]Met Office Hadley Centre, Met Office, Exeter, UK, [5]CECI CNRS-Cerfacs, Toulouse, France, [6]NCAS, School of Earth and the Environment, University of Leeds, Leeds, UK, [7]NOAA/GFDL, Princeton, NJ, USA

Key Points:
- The Atlantic Meridional Overturning Circulation (AMOC) is important in modulating climate change, but its past evolution is uncertain
- In CMIP6 historical runs, the AMOC strengthens by ~10% as a response to increased forcing from aerosol indirect effects, unlike in CMIP5
- Observational constraints suggest that anthropogenic forcing and/or the AMOC response may be overestimated

Supporting Information:
- Supporting Information S1

Correspondence to:
M. B. Menary,
matthew.menary@locean-ipsl.upmc.fr

Citation:
Menary, M. B., Robson, J., Allan, R. P., Booth, B. B. B., Cassou, C., & Gastineau, G., et al. (2020). Aerosol-forced AMOC changes in CMIP6 historical simulations. *Geophysical Research Letters*, *47*, e2020GL088166. https://doi.org/10.1029/2020GL088166

Received 27 MAR 2020
Accepted 15 JUN 2020
Accepted article online 8 JUL 2020

©2020. The Authors.
This is an open access article under the terms of the Creative Commons Attribution License, which permits use, distribution and reproduction in any medium, provided the original work is properly cited.

Abstract The Atlantic Meridional Overturning Circulation (AMOC) has been, and will continue to be, a key factor in the modulation of climate change both locally and globally. However, there remains considerable uncertainty in recent AMOC evolution. Here, we show that the multimodel mean AMOC strengthened by approximately 10% from 1850–1985 in new simulations from the 6th Coupled Model Intercomparison Project (CMIP6), a larger change than was seen in CMIP5. Across the models, the strength of the AMOC trend up to 1985 is related to a proxy for the strength of the aerosol forcing. Therefore, the multimodel difference is a result of stronger anthropogenic aerosol forcing on average in CMIP6 than CMIP5, which is primarily due to more models including aerosol-cloud interactions. However, observational constraints—including a historical sea surface temperature fingerprint and shortwave radiative forcing in recent decades—suggest that anthropogenic forcing and/or the AMOC response may be overestimated.

1. Introduction

The Atlantic Meridional Overturning Circulation (AMOC) represents the Atlantic branch of the global overturning circulation. It plays a significant role in both local and global climate, transporting heat from the South Atlantic to the North Atlantic and sequestering anthropogenic carbon in the deep ocean (Buckley & Marshall, 2016). Changes in the strength of the AMOC are thought to be an important driver of changes in North Atlantic sea surface temperature (SSTs) (Ba et al., 2014; Rahmstorf et al., 2015). Hence, changes in the AMOC strength could have important impacts on a range of far-reaching phenomena, including the number of hurricanes (Yan et al., 2017), Sahel drought (Zhang & Delworth, 2006), and Atlantic storm tracks (Woollings et al., 2012). In addition, the AMOC affects variability in Arctic sea-ice extent (Mahajan et al., 2011), which has also been linked with midlatitude climate variability (Screen et al., 2018).

Various lines of modeling and paleo-oceanographic evidence suggest the AMOC may weaken under the effects of greenhouse gases (GHGs) (Gregory et al., 2005; Stommel, 1961; Stouffer et al., 2006; Thornalley et al., 2018; Wood et al., 1999), leading to consistent projections that the AMOC will weaken in the next century (Collins et al., 2013). Such a weakening could have severe climate impacts (Jackson et al., 2015). Yet the AMOC is also thought to be sensitive to a range of other natural and anthropogenic external forcings (Menary & Scaife, 2014; Otterå et al., 2010; Swingedouw et al., 2015). In particular, increases in anthropogenic aerosol forcing are thought to have opposed GHG induced weakening over the 20th century (Cai et al., 2006; Delworth & Dixon, 2006). The Coupled Model Intercomparison Project Phase 5 (CMIP5) multimodel mean showed no net forced AMOC change over the historical period (Cheng et al., 2013), but some individual models did show a strong increase, which was attributed to aerosol forcing (Menary et al., 2013). There is large uncertainty in the simulated strength and spatial pattern of historical anthropogenic aerosol forcing, particularly due to their interaction with clouds (i.e., indirect effects) (Myhre et al., 2013). There is also considerable uncertainty in the future changes in anthropogenic aerosol emission and related forcing (Lund et al., 2019). Hence, given their potentially important role, the uncertainty in aerosol forcing could have implications for the interpretation of simulated historical AMOC variability, as well as its near future evolution. Thus, in this study, we revisit the simulation of historical AMOC changes in the new CMIP6 simulations.

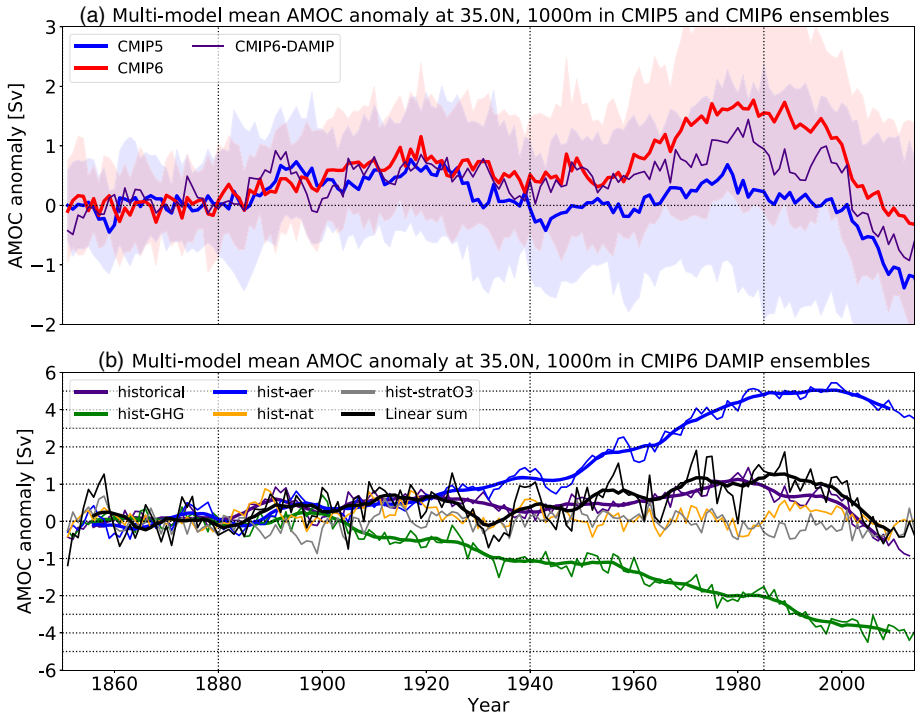

Figure 1. Historical AMOC change in CMIP. (a) AMOC time series in CMIP5 (blue, comprising 39 models and 128 ensemble members) and CMIP6 (red, comprising 25 models and 133 ensemble members) multimodel ensembles. Also shown is the subset of seven CMIP6 models with DAMIP experiments (purple). Shading highlights one standard deviation of the multimodel (anomaly) ensemble. (b) AMOC time series in DAMIP experiments. Lines show annual mean (thin) and 11-year running mean (thick). Note the non-linear *y*-axis for clarity. Thin purple lines in panels (a) and (b) are identical. Vertical dashed lines highlight endpoints of meaning periods (1850–1880) and trends (1940 and 1985) discussed in the main text.

2. Methods

We compare the evolution of the AMOC in historical simulations from CMIP5 and CMIP6. We also use historical simulations from the Detection and Attribution Model Intercomparison Project (DAMIP) (Gillett et al., 2016), which discriminate external forcing variability in greenhouse gases (GHGs; hist-GHG), anthropogenic aerosols (hist-aer), natural forcing (hist-nat), and changes in stratospheric ozone (hist-stratO3). The data we use are obtained from the relevant CMIP archives. The models included in this study are summarized in supporting information Table S1. We have used 39 models (totaling 128 members) from CMIP5, 25 (133 members) for CMIP6 and seven (45 members) for the CMIP6-DAMIP (counting only those models that have multiple ensemble members including at least both the "hist-GHG" and "hist-aer" experiments, at the time of writing). For CMIP5 analysis that extends after the end of the CMIP5 historical simulations we use scenario data from RCP8.5. When computing multimodel ensemble means as in Figure 1, we first compute the ensemble mean for each model (averaging over all realizations), before combining these into the grand ensemble mean, that is, 1-model, 1-vote. Averaging over all ensemble members and models simultaneously yields similar conclusions (i.e., 1-simulation, 1-vote, not shown).

In many cases, the variable used to store the Atlantic meridional overturning circulation stream function was not uploaded to the CMIP archives. As such, to increase our ensemble size, we instead use the oceanic meridional velocities and calculate the overturning stream function directly for each model. Where both meridional stream function and oceanic meridional velocities exist, the correlation between indices of annual AMOC variability at 35°N and 1,000 m depth are greater than $r = 0.96$ in all cases, giving us confidence in our approach (Figure S1). For consistency of approach, in all cases we use the stream function calculated from the meridional velocities. In many of the models, the velocity data do not exist on a regular latitude/longitude grid but becomes increasingly curved toward the North Pole. As such, we focus on 35°N as a balance between a northerly latitude and one where the true latitudes of the velocity grid lines

remain similar, enabling more precise calculation of the (true) meridional stream function in both online and our offline calculations (Table S1). However, although the timing and magnitude of temporal variability is well represented, we do find a spatially varying, but temporally constant, offset between our calculation of the AMOC stream function and the meridional stream function variable uploaded to CMIP (Figure S1). This is likely the result of using estimated, constant values for cell widths/heights (based on the model grid design) as well as potentially different masking choices. Therefore, we restrict our analysis to the temporal evolution of the AMOC, which is well captured by our method. We take temporal anomalies with respect to the period 1850–1880; the start of the period is chosen as the beginning of the historical simulations, and the end chosen to be before the first major eruption in these simulations (Krakatoa in 1883). Finally, note that, although the main results of this paper are focused on 35°N, similar results are found at 45°N or at 26.5°N where the RAPID observational array is located (Cunningham et al., 2007).

3. Results

3.1. Forced AMOC Variability in CMIP5 and CMIP6

The multimodel ensemble mean evolution of the AMOC anomaly at 35°N shows a significantly different evolution in the second half of the 20th century between CMIP5 and CMIP6 historical simulations (Figure 1a). CMIP6 shows a positive trend from 1850 to 1985 (1.0 Sv/century, $p < 0.01$) dominated by the strong trend from 1940 to 1985 (3.4 Sv/century), before a weakening (−7.6 Sv/century, 1985–2014). The AMOC peak in CMIP6 is around 1.6 Sv stronger (1980–1990 time mean, i.e., centered around the end of the trend period) than at the beginning of the historical simulations (1850–1880 mean). The increase to the 1980s represents a ~10% increase compared to time-mean observations at 26.5°N (Smeed et al., 2019) and is comparable to one intermodel standard deviation of the CMIP6 anomaly ensemble during this period (1.7 Sv). By comparison, the AMOC in CMIP5 is only around 0.2 Sv stronger. The multidecadal structure in CMIP5 resembles that of CMIP6, but the strengthening toward the end of the 20th century is far less pronounced. Finally, repeated subsampling of the larger CMIP5 ensemble (39 models) down to the current size of the CMIP6 ensemble (25 models) suggests the stronger trends in CMIP6 are unlikely to be due to the smaller sample size (Figure S2).

Analysis of the single-forcing experiments as part of DAMIP (Figure 1b) illustrates that the forced response of AMOC from 1850 to 1985 is a balance of opposing contributions from aerosols (increase) and greenhouse gases (decrease), consistent with previous work (Delworth & Dixon, 2006). Summing the AMOC anomalies from the various single-forcing experiments shows that for the 1980s mean the AMOC peak is dominated by the aerosol-forced increase. Note that in the subsampled subset of models where both historical and DAMIP simulations are available, the evolution of the AMOC is similar to the full CMIP6 ensemble, albeit that the peak in the 1980s is weaker (1.0 Sv compared to 1.6 Sv, see Figure 1a). The annual and decadal mean correlations between the subsampled historical and linear sum are $r = 0.53$ and $r = 0.81$, respectively ($p < 0.01$ for both), suggesting that the forcings are additive, as the linear sum captures the key features (more than half of the variance) of at least the longer timescale variability (Figure 1b). Within this linear framework, the decline in the AMOC following its peak in the 1980s can be attributed to a leveling off of the rate of change of global aerosol optical depth (Booth et al., 2012) (and the associated aerosol-driven AMOC strengthening) while the GHG-driven weakening continues unabated, although long-timescale feedbacks with the Arctic could also play a role (Jungclaus et al., 2005).

3.2. Relationship Between AMOC Changes and the Strength of the Aerosol Forcing

To investigate further the relationship between the strength of the aerosol forcing and the forced AMOC trends we define an index based on the total absorbed solar radiation (ASR; i.e., the net top of atmosphere shortwave [SW] radiation). As historical anthropogenic aerosol emissions have primarily been in the northern hemisphere, we subsequently take the difference between southern and northern hemispheres (southern minus northern) to focus on the relative aerosol forcing of the northern hemisphere (ASR_HD: ASR hemispheric difference). We use this index, rather than estimates based on atmosphere-only simulations, as it provides a time-dependent estimate of the strength of the aerosol forcing, and it can be estimated in any simulation, that is, it is not dependent on the availability of other tailored simulations.

The ASR_HD index will be sensitive to any processes that drive hemispheric changes in ASR, including both hemispheric differences in anthropogenic and natural (e.g., volcanic) aerosols but also climate feedbacks,

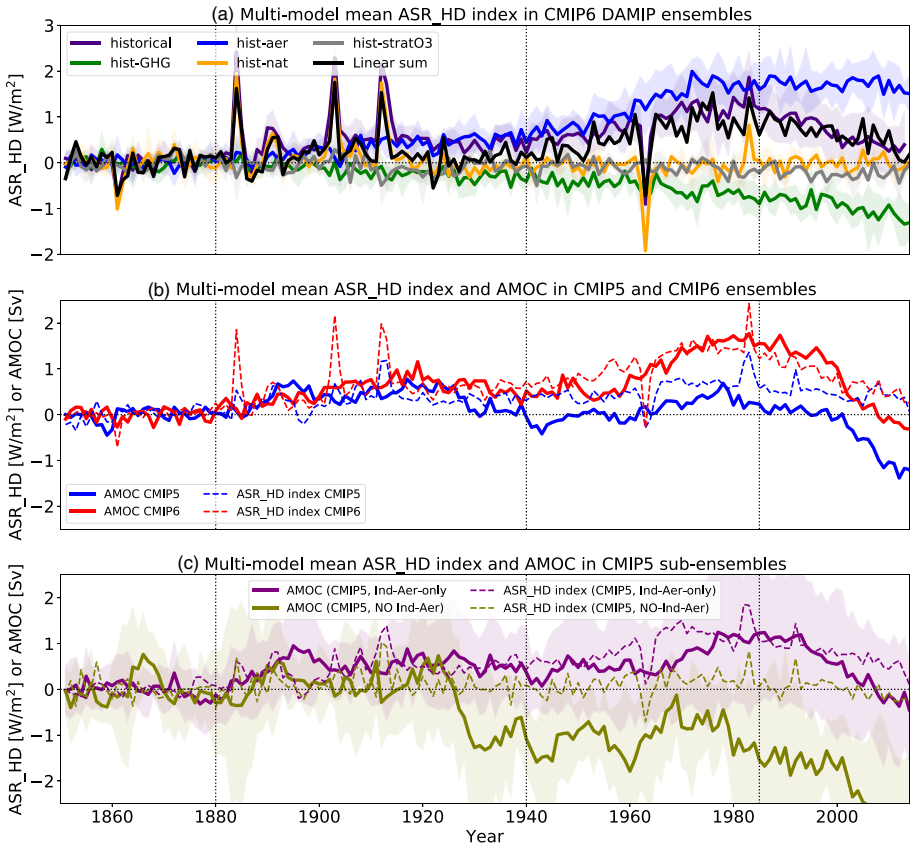

Figure 2. The relationship between ASR_HD index and the AMOC. (a) Time series of hemispheric imbalance in absorbed solar radiation (ASR_HD) index in CMIP6 DAMIP. Purple shows the time series from the subsampled historical runs with the same models. Shading shows multimodel one standard deviation. (b) AMOC and ASR_HD index in CMIP5 and CMIP6 multimodel ensembles. (c) AMOC and ASR_HD in two subsets of CMIP5: Models explicitly using aerosol indirect effects (purple, 15 models), and models that explicitly are not (green, 10 models) after Wilcox et al. (2013). Vertical dashed lines highlight endpoints of meaning periods (1850–1880) and trends (1940 and 1985) discussed in the main text.

such as changes in ice and land albedo and clouds. Nonetheless, trends in this ASR_HD index compare well ($r = 0.90$, $p < 0.01$) with published estimates of the northern hemisphere historical aerosol present-day versus preindustrial radiative forcing determined from independent time-slice experiments with prescribed sea surface temperatures in CMIP5 (Booth et al., 2018) (Figure S3). In addition, within the CMIP6-DAMIP ensemble, changes in the ASR_HD index from 1850 to 1985 (i.e., the peak AMOC; Figure 2a) are dominated by the increase seen in the hist-aer experiment. Furthermore, as with the AMOC time series, the sum of the ASR_HD index anomalies in the individual DAMIP experiments is a good approximation of the evolution in the historical experiment, giving us confidence in the additivity of the dominant GHG and aerosol forcings. Thus we are confident that the ASR_HD index is related to the magnitude of aerosol forcing up to 1985.

We now compare the ASR_HD index in both the CMIP5 and CMIP6 ensembles (Figure 2b). The CMIP6 1980–1990 multimodel mean ASR_HD index increased by 1.42 W/m^2, which is larger than CMIP5 (0.73 W/m^2), suggesting that aerosol forcing is stronger in CMIP6. In CMIP6, the multidecadal evolution of the index over the period 1850–1985 is well correlated with the ensemble multimodel mean AMOC ($r = 0.96$ for decadal correlations compared to $r = 0.76$ for annual correlations, with maximum correlation when the ASR_HD index leads the AMOC index by 2–4 years; $p < 0.01$). However, in CMIP5, the multimodel mean AMOC and multimodel mean ASR_HD indices diverge in the 20th century. As a result, the correlation between the time series in CMIP5 is $r = 0.48$ for decadal timescales. Thus, this could suggest that the

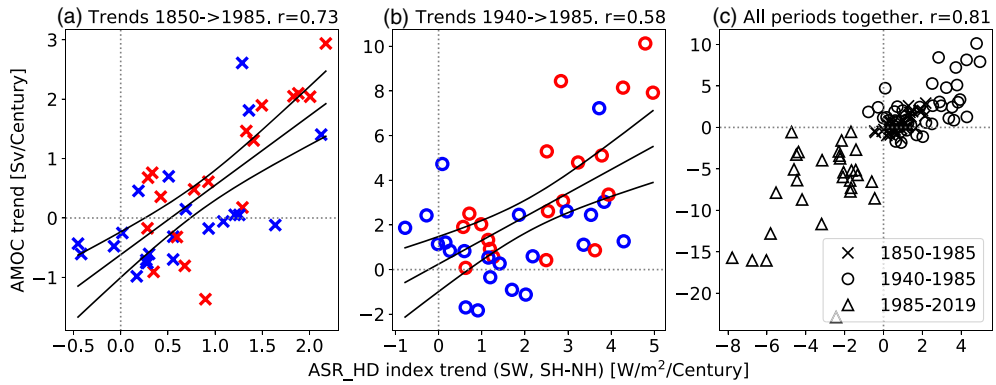

Figure 3. ASR_HD index trend (*x*-axis) versus AMOC trend (*y*-axis) for different epochs (a: 1850 to >1985, b: 1940 to >1985, c: all periods together [1850–1985, 1940–1985, and 1985–2014]). Red: CMIP6. Blue: CMIP5. Black lines denote a linear fit along with 95% confidence intervals on this slope.

AMOC response to that forcing is weaker in CMIP5 allowing other forcings, such as GHG-driven AMOC weakening to dominate. It may also reflect the conflation of CMIP5 models with and without important aerosol processes, discussed next.

Despite the lack of CMIP5 multimodel mean AMOC strengthening, we do find a strong dependency of forced AMOC trends on the inclusion of aerosol-cloud interactions (or indirect effects) in CMIP5. Aerosol-schemes within climate models have undergone significant development in recent years, in particular with regard to these effects (Rosenfeld et al., 2014) such that all the CMIP6 models considered here include some representation of aerosol indirect effects, which was not the case in CMIP5. When considering only those CMIP5 models that included both direct and indirect effects (as diagnosed in Wilcox et al. (2013), we find that the increase in ASR_HD is larger than the CMIP5 mean value (1.20 W/m^2; see Figure 2c) and that the multidecadal evolution of the AMOC compares well to the ASR_HD index with decadal correlations of (r = 0.80). The AMOC anomaly for the decade 1980–1990 is 1.14 Sv. Conversely, considering only those models where indirect effects were not included, the change in the ASR_HD is small (0.15 W/m^2) and the AMOC actually weakens throughout the 20th century, resulting in no temporal correlation between the multimodel mean ASR_HD index and multimodel mean AMOC (r = 0.03). In this sub-ensemble, the ASR_HD index remains relatively flat, suggesting that the indirect aerosol effect dominates the ASR_HD index variability, as also seen in dedicated experiments (Zelinka et al., 2014).

So far, we have focused on multimodel ensemble means in our analysis, but we also find that the strength of the forced AMOC trend from 1850 to 1985 is systematically related to the ASR_HD index across individual models. Figures 3a and 3b show the 1850–1985 and 1940–1985 ensemble mean trends in the ASR_HD index and AMOC indices for each model. When considering all CMIP5 and CMIP6 models together, the correlation between the trends in AMOC and in ASR_HD over the periods 1850–1985 and 1940–1985 are r = 0.73 and r = 0.58, respectively. For the period 1850–1985, there is a general relationship between AMOC and SW forcing *trends* with models with a strong increase in ASR_HD having a strong increase in AMOC, and vice versa. Furthermore, for the period 1850–1985, the correlations for either CMIP5 or CMIP6 alone are both significant (at the 5% level for a two-tailed *t*-test). However, for the more rapid 20th century strengthening (1940–1985) this represents a balance between the CMIP5 ensemble, where a significant relationship is not found (r = 0.27) and the CMIP6 ensemble, where the relationship is much stronger (r = 0.73). This could indicate that the stronger aerosol forcing is dominating internal variability in CMIP6 but could also reflect the signal-to-noise issues when using the smaller ensemble sizes typically used with CMIP5 models (see Table S1).

3.3. Comparison With SST-Based AMOC Estimates

An important question is whether the long-term AMOC behavior in CMIP6 is consistent with the real world AMOC. Unfortunately, direct AMOC observations only exist at 26.5°N since 2004, and so indirect constraints are needed. Notably, the multimodel mean CMIP6 historical AMOC strengthening is different to recently reported AMOC weakening during the 20th century (Rahmstorf et al., 2015). That result was

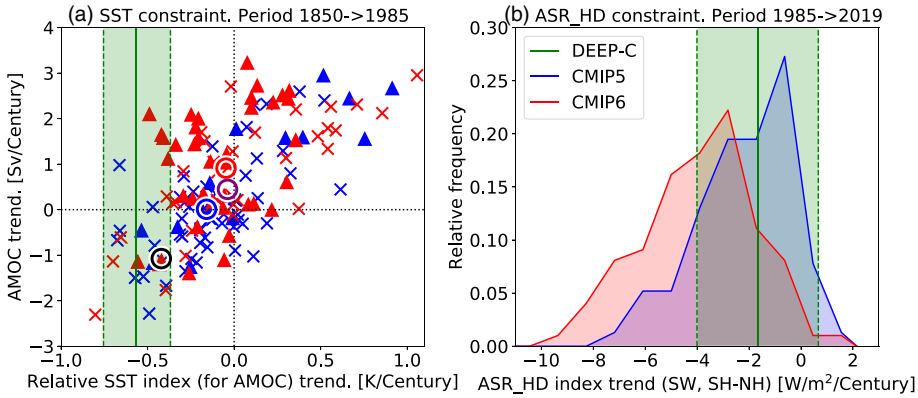

Figure 4. (a) Relationship between AMOC and relative SPNA SST fingerprint (based on Rahmstorf et al., 2015, and Caesar et al., 2018) and the AMOC trend in all ensemble members (1–10) in all available models. Symbols represent ensemble members that exist within (crosses) and outside of (triangles) the independent ASR_HD observational estimate shown in panel (b). Red: CMIP6, blue: CMIP5. Circles: Multimodel ensemble mean of each sub-ensemble, which includes CMIP5 models including indirect aerosol effects (purple) and CMIP5 not including indirect aerosol effects (black). Vertical line and shading (green) show same fingerprint from HadISST and 95% confidence interval on the trend. (b) ASR_HD trends over the recent, observed period (1985–2019) shown as a probability density function in CMIP5 (blue) and CMIP6 (red) using all relevant ensemble members. Vertical line and shading (green) show the trend from DEEP-C observations and 95% confidence interval on the trend. Note the slightly later endpoint (2019), which was chosen to maximize the available observational data. Simulated trends are computed only when there are data for >90% of the period, requiring scenario data for CMIP5 (see section 2).

based largely on the AMOC/SST relationship in a subset of CMIP5 climate models. Specifically, they show that there is a positive correlation between subpolar North Atlantic (SPNA) SST and AMOC, after the subpolar SST has been detrended by removing either northern hemisphere surface air temperatures (Rahmstorf et al., 2015) or global mean SSTs (November to May means) (Caesar et al., 2018). Therefore, given the differences in AMOC between CMIP5 and CMIP6, it seems appropriate to revisit such SST-based AMOC indices. In the subsequent analysis, we define the relative SPNA SST index as annual mean, SPNA mean (20–55°W, 46–60°N) SSTs minus annual mean, global mean SSTs.

Figure 4a shows that there is a systematic relationship between trends in AMOC and relative SPNA anomalies across both CMIP5 and CMIP6 models using individual ensemble members ($r = 0.70$). Generally, model simulations with the strongest increase in AMOC over the 1850–1985 period tend to show a warming of the SPNA relative to the rest of the globe, whereas models with a weakening AMOC show a relative cooling. This relationship also holds for the multimodel means; the CMIP6 model mean, which had the strongest AMOC increase, shows little SPNA change, whereas CMIP5 models that do not include aerosol indirect effects show a strong relative cooling of the SPNA.

Also plotted in Figure 4a is an observed estimate computed from HadISST (vertical green line), which shows a relative cooling (robust uncertainty estimates are hard to generate for the observations; here we simply use the statistical uncertainty on the trend assuming no observational error). The SPNA trend is furthest from the observational estimate in those models that have the strongest, aerosol-forced, increase in AMOC (both ensemble mean values and individual members). Therefore, the comparison in Figure 4 could suggest that in some models either the aerosol forcing is too strong or that the AMOC responds too strongly to that forcing. Such an increase in the strength of anthropogenic aerosol forcing in CMIP6 relative to CMIP5 would be concerning given that it may already have been too strong in CMIP5 (Gregory et al., 2019). However, uncertainty in aerosol forcing remains large (Bellouin et al., 2020), and we will discuss later that the relative SPNA SST index may not be well designed to capture historically forced AMOC variability and change.

4. Discussion

In this paper we have shown that the multimodel mean AMOC in CMIP6 increases by ~10% from 1850 to the 1980s, in contrast to the CMIP5 multimodel mean, which shows little change over this time period. We have

used single-forcing experiments, in particular historical anthropogenic aerosols, to diagnose the important external forcing. Finally, by exploring an index of interhemispheric imbalances in total absorbed solar radiation (ASR_HD), we show that the AMOC increase in CMIP6 is due to the inclusion of more models with a stronger aerosol forcing than in CMIP5 and particularly the inclusion of indirect aerosol forcing.

We have focused most of the analysis on trends in the AMOC and ASR_HD up to 1985, using ASR_HD as a proxy of aerosol forcing. There is a weaker relationship for the 1985–2014 period, but it remains consistent with the long-term correlation between ASR_HD and AMOC (Figure 3c). The weaker relationship in the 1985–2014 period may reflect the smaller number of simulations available (scenario data are required for the CMIP5 models) or the shorter time period used but may also be linked to the GHG-driven AMOC weakening. When considering the temporal evolution over the whole 1850–2014 period, the correlation between the decadal smoothed CMIP6 multimodel mean time series of AMOC and ASR_HD shown in Figure 2a is 0.95. The peak multimodel mean ASR_HD in the 1980s is equivalent to a 0.4 PW hemispheric imbalance with respect to 1850–1880 but is greater than 0.7 PW for models with the strongest response. As the AMOC plays an important role in the cross-equator heat transport (Frierson et al., 2013), one interpretation is that the forced changes in the AMOC are consistent with interhemispheric top of atmosphere (TOA) energy constraints (Yu & Pritchard, 2019). However, there remains considerable uncertainty in the simulation of interhemispheric energy imbalances (see Figure S4), and we cannot rule out that more Atlantic-centric mechanisms are at play (Ceppi et al., 2014; Delworth & Dixon, 2006; Menary et al., 2013). Therefore, the mechanisms of forced AMOC changes in CMIP6 will need to be studied further in future work.

Although observational TOA diagnostics are not available for the whole of the historical period, they are available for the 1985–2019 period using DEEP-C estimates combining the ERBE and CERES data (Allan et al., 2014). Figure 4b shows that the (negative) trends in ASR_HD may be overestimated in some models when compared to the observations, with 55% of ensemble members in CMIP6 (and 20% of ensemble members in CMIP5) outside of the 95% confidence intervals on the observed trend, consistent with biases in cross-equatorial atmospheric heat transport previously seen in CMIP5 (Loeb et al., 2016). Given the strong relationship between ASR_HD and AMOC, this could suggest that many models, and in particular CMIP6 models, would also overestimate the changes in AMOC over this time period. However, there could be other important implications: Single-forcing experiments (DAMIP) indicate that greenhouse gas forcing dominates the decline in ASR_HD from 1985 in historical simulations (see Figure 2a), presumably through cloud and surface albedo feedbacks (i.e., Arctic amplification). However, restricting the computation of the ASR_HD index to 60°S–60°N (i.e., removing regions with strong ice albedo feedbacks) makes little difference to the ASR_HD in hist-GHG (not shown). Therefore, the overestimation of ASR_HD could indicate not only that the interhemispheric response to GHGs might be too large in many models but also that cloud feedbacks are too large or exhibit the wrong asymmetry as well as uncertainties in continental surface albedo (Levine & Boos, 2017). Nonetheless, there is also considerable uncertainty with observed estimates of ASR_HD (Allan et al., 2014), and further study is required.

As noted above, there are also uncertainties in the relationship between the relative SPNA SST index and AMOC. For example, it is not clear whether the relationship between the relative SPNA SST index and AMOC is stationary in time or with regard to the forcing. For the subset of models used in Caesar et al. (2018) the correlation of trends over the 1850–1985 reduces from $r = 0.65$ when using the first ensemble member to $r = -0.11$ when using available ensemble means (i.e., the forced signal; Figure S5). There also remains significant diversity in the patterns of simulated historical SST trends, as with future projections with CMIP5 models (Menary & Wood, 2018). As such, the interpretation of the forced AMOC response using the relative SPNA SST index is challenging. In addition, models that are deemed less plausible via the more recent ASR_HD constraint (Figure 4b) are not necessarily outliers when considered against the longer-term SPNA SST index (triangles in Figure 4a). Further investigation of this index could involve analysis of preindustrial control simulations without interannually varying external forcings.

Finally, there are a number of further caveats that deserve discussion. We showed that the inclusion of aerosol indirect effects appeared to account for around two thirds of the difference between CMIP5 and CMIP6 multimodel mean AMOC changes (between 1980–1990 and 1850–1880). The remaining fraction may be the result of increased aerosol emissions, and changes in their distribution, in CMIP6 versus CMIP5, or changes

in the precise representation of aerosol effects in models, but we are unable to diagnose this effect in our analysis. The spatial pattern of aerosol forcing may have changed regionally between CMIP5 and CMIP6—especially indirect effects (Chung & Soden, 2017; Zelinka et al., 2014)—which could be important for the forced response (Yu & Pritchard, 2019). Other forcing agents (e.g., volcanoes) may also play a role (Swingedouw et al., 2015), and the response to forcing is likely to be model dependent. There is also significant uncertainty about the role of internal variability versus external forcing. For example, there is evidence that decadal timescale AMOC variability is underestimated in CMIP5 models (Kim et al., 2017; Roberts et al., 2014; Yan et al., 2018). Furthermore, past AMOC variability has been linked to other mechanisms (e.g., decadal variability in the NAO; Robson et al., 2012). In particular, ocean-only simulations initialized in 1960 often demonstrate an AMOC minima around 1970 and a peak AMOC around 2000, linked with NAO variability (Tsujino et al., 2020; Xu et al., 2019). In addition, some multidecadal oceanic responses to (indirect) aerosol forcing have been suggested to be spurious (Zhang et al., 2013), and recent observational and cloud-resolving modeling studies have also suggested that the indirect aerosol effect might have been overestimated in many climate models (Sato et al., 2018; Toll et al., 2019). As such, further, detailed, multivariate, evaluation of CMIP6 simulations against observations is needed to understand the veracity of the forced response in CMIP6.

Data Availability Statement

The climate model simulations are available via the Earth System Grid Federation (ESGF) archive of Coupled Model Intercomparison Project 6 (CMIP6) data (https://esgf-index1.ceda.ac.uk/projects/esgf-ceda/).

Acknowledgments

M. B. M. was supported by the EPICE project funded by the European Union's Horizon 2020 programme, Grant Agreement 789445. J. R., D. H., and R. S. were supported by the National Environmental Research Council (NERC) "North Atlantic Climate System Integrated Study" (ACSIS) program and NCAS. J. G. was supported by NERC via NCAS. C. J. was supported by the NERC national capability grant for UK Earth System Modelling, NE/N017951/1 and by the EU Horizon 2020 Research Programme CRESCENDO project, Grant Agreement 641816. B. B. B. B. and M. R. were supported by the Joint UK BEIS/Defra Met Office Hadley Centre Climate Programme (GA01101). L. J. W. was supported by the Natural Environment Research Council (NERC) as part of the SMURPHS and EMERGENCE projects (NE/N006054/1 and NE/S004890/1). We thank Mike Winton and Ming Zhao and two anonymous reviewers for their comments on the manuscript.

References

Allan, R. P., Liu, C., Loeb, N. G., Palmer, M. D., Roberts, M., Smith, D., & Vidale, P.-L. (2014). Changes in global net radiative imbalance 1985–2012. *Geophysical Research Letters*, *41*, 5588–5597. https://doi.org/10.1002/2014GL060962

Ba, J., Keenlyside, N. S., Latif, M., Park, W., Ding, H., Lohmann, K., et al. (2014). A multi-model comparison of Atlantic multidecadal variability. *Climate Dynamics*, *43*(9-10), 2333–2348. https://doi.org/10.1007/s00382-014-2056-1

Bellouin, N., Quaas, J., Gryspeerdt, E., Kinne, S., Stier, P., Watson-Parris, D., et al. (2020). Bounding global aerosol radiative forcing of climate change. *Reviews of Geophysics*, *58*. https://doi.org/10.5194/egusphere-egu2020-7745

Booth, B., Dunstone, N., Halloran, P., Bellouin, N., & Andrews, T. (2012). Aerosols implicated as a prime driver of twentieth-century North Atlantic climate variability. *Nature*, *484*, 228–232. https://doi.org/10.1038/nature10946

Booth, B. B. B., Harris, G. R., Jones, A., Wilcox, L., Hawcroft, M., & Carslaw, K. S. (2018). Comments on "rethinking the lower bound on aerosol radiative forcing". *Journal of Climate*, *31*, 9407–9412. https://doi.org/10.1175/jcli-d-17-0369.1

Buckley, M. W., & Marshall, J. (2016). Observations, inferences, and mechanisms of the Atlantic meridional overturning circulation: A review. *Reviews of Geophysics*, *54*, 5–63. https://doi.org/10.1002/2015RG000493

Caesar, L., Rahmstorf, S., Robinson, A., Feulner, G., & Saba, V. (2018). Observed fingerprint of a weakening Atlantic Ocean overturning circulation. *Nature*, *556*, 191–196. https://doi.org/10.1038/s41586-018-0006-5

Cai, W., Bi, D., Church, J., Cowan, T., Dix, M., & Rotstayn, L. (2006). Pan-oceanic response to increasing anthropogenic aerosols: Impacts on the Southern Hemisphere oceanic circulation. *Geophysical Research Letters*, *33*, L21707. https://doi.org/10.1029/2006GL027513

Ceppi, P., Zelinka, M. D., & Hartmann, D. L. (2014). The response of the Southern Hemispheric eddy-driven jet to future changes in shortwave radiation in CMIP5. *Geophysical Research Letters*, *41*, 3244–3250. https://doi.org/10.1002/2014gl060043

Cheng, W., Chiang, J. C. H., & Zhang, D. (2013). Atlantic meridional overturning circulation (AMOC) in CMIP5 models: RCP and historical simulations. *Journal of Climate*, *26*, 7187–7197. https://doi.org/10.1175/jcli-d-12-00496.1

Chung, E.-S., & Soden, B. J. (2017). Hemispheric climate shifts driven by anthropogenic aerosol–cloud interactions. *Nature Geoscience*, *10*, 566–571. https://doi.org/10.1038/ngeo2988

Collins, M., Knutt, R., Arblaster, J., Dufresne, J.-L., Fichefet, T., Friedlingstein, P., et al. (2013). Long-term climate change: Projections, commitments and irreversibility. In T. F. Stocker, D. Qin, G.-K. Plattner, M. Tignor, S. K. Allen, J. Boschung, A. Nauels, Y. Xia, V. Bex, & P. M. Midgley. *Climate change: The physical science basis*. Contribution of Working Group I to the Fifth Assessment Report of the Intergovernmental Panel on Climate Change *Contribution of Working Group I to the Fifth Assessment Report of the Intergovernmental Panel on Climate Change*. Cambridge, UK; New York, NY: Cambridge University Press.

Cunningham, S. A., Kanzow, T., Rayner, D., Baringer, M. O., Johns, W. E., Marotzke, J., et al. (2007). Temporal variability of the Atlantic meridional overturning circulation at 26.5N. *Science*, *317*, 935–938. https://doi.org/10.1126/science.1141304

Delworth, T. L., & Dixon, K. W. (2006). Have anthropogenic aerosols delayed a greenhouse gas-induced weakening of the North Atlantic thermohaline circulation? *Geophysical Research Letters*, *33*, L02606. https://doi.org/10.1029/2005GL024980

Frierson, D. M. W., Hwang, Y.-T., Fučkar, N. S., Seager, R., Kang, S. M., Donohoe, A., et al. (2013). Contribution of ocean overturning circulation to tropical rainfall peak in the Northern Hemisphere. *Nature Geoscience*, *6*, 940–944. https://doi.org/10.1038/ngeo1987

Gillett, N. P., Shiogama, H., Funke, B., Hegerl, G., Knutti, R., Matthes, K., et al. (2016). The Detection and Attribution Model intercomparison Project (DAMIP v1.0) contribution to CMIP6. *Geoscientific Model Development*, *9*, 3685–3697. https://doi.org/10.5194/gmd-9-3685-2016

Gregory, J., Dixon, K. W., Stouffer, R. J., Weaver, A. J., Driesschaert, E., Eby, M., et al. (2005). A model intercomparison of changes in the Atlantic thermohaline circulation in response to increasing atmospheric CO_2 concentration. *Geophysical Research Letters*, *32*, L12703. https://doi.org/10.1029/2005GL023209

Gregory, J. M., Andrews, T., Ceppi, P., Mauritsen, T., & Webb, M. J. (2019). How accurately can the climate sensitivity to CO_2 be estimated from historical climate change? *Climate Dynamics*, *54*. https://doi.org/10.1007/s00382-019-04991-y

Jackson, L., Kahana, R., Graham, T., Ringer, M. A., Woollings, T., Mecking, J. V., & Wood, R. A. (2015). Global and European climate impacts of a slowdown of the AMOC in a high resolution GCM. *Climate Dynamics*, *45*, 3299–3316. https://doi.org/10.1007/s00382-015-2540-2

Jungclaus, J., Haak, H., Latif, M., & Mikolajewicz, U. (2005). Arctic-North Atlantic interactions and multidecadal variability of the meridional overturning circulation. *Journal of Climate*, *18*, 4013–4031. https://doi.org/10.1175/jcli3462.1

Kim, W. M., Yeager, S., Chang, P., & Danabasoglu, G. (2017). Low-frequency North Atlantic climate variability in the community earth system model large ensemble. *Journal of Climate*, *31*, 787–813. https://doi.org/10.1175/jcli-d-17-0193.1

Levine, X. J., & Boos, W. R. (2017). Land surface albedo bias in climate models and its association with tropical rainfall. *Geophysical Research Letters*, *44*, 6363–6372. https://doi.org/10.1002/2017GL072510

Loeb, N. G., Wang, H., Cheng, A., Kato, S., Fasullo, J. T., Xu, K.-M., & Allan, R. P. (2016). Observational constraints on atmospheric and oceanic cross-equatorial heat transports: Revisiting the precipitation asymmetry problem in climate models. *Climate Dynamics*, *46*, 3239–3257. https://doi.org/10.1007/s00382-015-2766-z

Lund, M. T., Myhre, G., & Samset, B. H. (2019). Anthropogenic aerosol forcing under the shared socioeconomic pathways. *Atmospheric Chemistry and Physics*, *19*, 13,827–13,839. https://doi.org/10.5194/acp-19-13827-2019

Mahajan, S., Zhang, R., & Delworth, T. L. (2011). Impact of the Atlantic meridional overturning circulation (AMOC) on Arctic surface air temperature and sea ice variability. *Journal of Climate*, *24*, 6573–6581. https://doi.org/10.1175/2011jcli4002.1

Menary, M. B., Roberts, C. D., Palmer, M. D., Halloran, P. R., Jackson, L., Wood, R. A., et al. (2013). Mechanisms of aerosol-forced AMOC variability in a state of the art climate model. *Journal of Geophysical Research: Oceans*, *118*, 2087–2096. https://doi.org/10.1002/jgrc.20178

Menary, M. B., & Scaife, A. A. (2014). Naturally forced multidecadal variability of the Atlantic meridional overturning circulation. *Climate Dynamics*, *42*, 1347–1362. https://doi.org/10.1007/s00382-013-2028-x

Menary, M. B., & Wood, R. A. (2018). An anatomy of the projected North Atlantic warming hole in CMIP5 models. *Climate Dynamics*, *50*, 3063–3080. https://doi.org/10.1007/s00382-017-3793-8

Myhre, G., Shindell, D., Bréon, F.-M., Collins, W., Fuglestvedt, J., Huang, J., et al. (2013). Anthropogenic and natural radiative forcing. In T. F. Stocker, et al. (Eds.), *Climate change: The physical science basis*. Contribution of Working Group I to the Fifth Assessment Report of the Intergovernmental Panel on Climate Change *Contribution of Working Group I to the Fifth Assessment Report of the Intergovernmental Panel on Climate Change*, Cambridge, UK; New York, NY: Cambridge University Press.

Otterå, O. H., Bentsen, M., Drange, H., & Suo, L. (2010). External forcing as a metronome for Atlantic multidecadal variability. *Nature Geoscience*, *3*, 688–694. https://doi.org/10.1038/ngeo955

Rahmstorf, S., Box, J. E., Feulner, G., Mann, M. E., Robinson, A., Rutherford, S., & Schaffernicht, E. J. (2015). Exceptional twentieth-century slowdown in Atlantic Ocean overturning circulation. *Nature Climate Change*, *5*(5), 475–480. https://doi.org/10.1038/nclimate2554

Roberts, C. D., Jackson, L., & McNeall, D. (2014). Is the 2004–2012 reduction of the Atlantic meridional overturning circulation significant? *Geophysical Research Letters*, *41*, 3204–3210. https://doi.org/10.1002/2014GL059473

Robson, J., Sutton, R., Lohmann, K., Smith, D., & Palmer, M. D. (2012). Causes of the rapid warming of the North Atlantic Ocean in the mid-1990s. *Journal of Climate*, *25*, 4116–4134. https://doi.org/10.1175/jcli-d-11-00443.1

Rosenfeld, D., Sherwood, S., Wood, R., & Donner, L. (2014). Climate effects of aerosol-cloud interactions. *Science*, *343*, 379–380. https://doi.org/10.1126/science.1247490

Sato, Y., Goto, D., Michibata, T., Suzuki, K., Takemura, T., Tomita, H., & Nakajima, T. (2018). Aerosol effects on cloud water amounts were successfully simulated by a global cloud-system resolving model. *Nature Communications*, *9*, 985. https://doi.org/10.1038/s41467-018-03379-6

Screen, J. A., Deser, C., Smith, D. M., Zhang, X., Blackport, R., Kushner, P. J., et al. (2018). Consistency and discrepancy in the atmospheric response to Arctic sea-ice loss across climate models. *Nature Geoscience*, *11*(3), 155–163. https://doi.org/10.1038/s41561-018-0059-y

Smeed, D., Moat, B. I., Rayner, D., Johns, W. E., Baringer, M. O., Volkov, D. L., & Frajka-Williams, E. (2019). *Atlantic meridional overturning circulation observed by the RAPID-MOCHA-WBTS (RAPID-Meridional Overturning Circulation and Heatflux Array-Western Boundary Time Series) array at 26N from 2004 to 2018*. Liverpool, UK: British Oceanographic Data Centre, National Oceanography Centre, NERC. https://www.bodc.ac.uk/data/published_data_library/catalogue/10.5285/8cd7e7bb-9a20-05d8-e053-6c86abc012c2/

Stommel, H. (1961). Thermohaline convection with two stable regimes of flow. *Tellus*, *13*, 224–230. https://doi.org/10.3402/tellusa.v13i2.9491

Stouffer, R. J., Yin, J., Gregory, J. M., Dixon, K. W., Spelman, M. J., Hurlin, W., et al. (2006). Investigating the causes of the response of the thermohaline circulation to past and future climate changes. *Journal of Climate*, *19*(8), 1365–1387. https://doi.org/10.1175/JCLI3689.1

Swingedouw, D., Ortega, P., Mignot, J., Guilyardi, E., Masson-Delmotte, V., Butler, P. G., et al. (2015). Bidecadal North Atlantic Ocean circulation variability controlled by timing of volcanic eruptions. *Nature Communications*, *6*. https://doi.org/10.1038/ncomms7545

Thornalley, D. J., Oppo, D. W., Ortega, P., Robson, J. I., Brierley, C. M., Davis, R., et al. (2018). Anomalously weak Labrador Sea convection and Atlantic overturning during the past 150 years. *Nature*, *556*(7700), 227–230. https://doi.org/10.1038/s41586-018-0007-4

Toll, V., Christensen, M., Quaas, J., & Bellouin, N. (2019). Weak average liquid-cloud-water response to anthropogenic aerosols. *Nature*, *572*, 51–55. https://doi.org/10.1038/s41586-019-1423-9

Tsujino, H., Urakawa, L. S., Griffies, S. M., Danabasoglu, G., Adcroft, A. J., Amaral, A. E., et al. (2020). Evaluation of global ocean–sea-ice model simulations based on the experimental protocols of the Ocean Model Intercomparison Project phase 2 (OMIP-2). *Geoscientific Model Development Discussion*, *2020*, 1–86. https://doi.org/10.5194/gmd-2019-363

Wilcox, L. J., Highwood, E. J., & Dunstone, N. J. (2013). The influence of anthropogenic aerosol on multi-decadal variations of historical global climate. *Environmental Research Letters*, *8*, 024033. https://doi.org/10.1088/1748-9326/8/2/024033

Wood, R. A., Keen, A. B., Mitchell, J. F., & Gregory, J. M. (1999). Changing spatial structure of the thermohaline circulation in response to atmospheric CO_2 forcing in a climate model. *Nature*, *399*, 572–575. https://doi.org/10.1038/21170

Woollings, T., Gregory, J. M., Pinto, J. G., Reyers, M., & Brayshaw, D. J. (2012). Response of the North Atlantic storm track to climate change shaped by ocean–atmosphere coupling. *Nature Geoscience*, *5*, 313–317. https://doi.org/10.1038/ngeo1438

Xu, X., Chassignet, E. P., & Wang, F. (2019). On the variability of the Atlantic meridional overturning circulation transports in coupled CMIP5 simulations. *Climate Dynamics*, *52*, 6511–6531. https://doi.org/10.1007/s00382-018-4529-0

Yan, X., Zhang, R., & Knutson, T. R. (2017). The role of Atlantic overturning circulation in the recent decline of Atlantic major hurricane frequency. *Nature Communications*, *8*, 1–8. https://doi.org/10.1038/s41467-017-01377-8

Yan, X., Zhang, R., & Knutson, T. R. (2018). Underestimated AMOC variability and implications for AMV and predictability in CMIP models. *Geophysical Research Letters*, *45*, 4319–4328. https://doi.org/10.1029/2018GL077378

Yu, S., & Pritchard, M. S. (2019). A strong role for the AMOC in partitioning global energy transport and shifting ITCZ position in response to Latitudinally discrete solar forcing in CESM1.2. *Journal of Climate*, *32*, 2207–2226. https://doi.org/10.1175/jcli-d-18-0360.1

Zelinka, M. D., Andrews, T., Forster, P. M., & Taylor, K. E. (2014). Quantifying components of aerosol-cloud-radiation interactions in climate models. *Journal of Geophysical Research: Atmospheres*, *119*, 7599–7615. https://doi.org/10.1002/2014JD021710

Zhang, R., & Delworth, T. L. (2006). Impact of Atlantic multidecadal oscillations on India/Sahel rainfall and Atlantic hurricanes. *Geophysical Research Letters*, *33*, L17712. https://doi.org/10.1029/2006GL026267

Zhang, R., Delworth, T. L., Sutton, R., Hodson, D. L. R., Dixon, K. W., Held, I. M., et al. (2013). Have aerosols caused the observed Atlantic multidecadal variability? *Journal of the Atmospheric Sciences*, *70*, 1135–1144. https://doi.org/10.1175/jas-d-12-0331.1